Journal of Applied Polymer Science

Isothermal Crystallization Kinetics of Poly(lactic acid)/Synthetic Mica Nanocomposites

Diego H. S. Souza, Cristina T. Andrade, Marcos L. Dias
Universidade Federal do Rio de Janeiro (UFRJ), Instituto de Macromoléculas Professora Eloisa Mano (IMA), Av. Horácio Macedo, 2.030, Centro de Tecnologia, BL J. 21941-598 Rio de Janeiro, Brazil
Correspondence to: M.L. Dias (E-mail: mldias@ima.ufrj.br)

ABSTRACT: The isothermal crystallization kinetics of PLA/fluoromica nanocomposites was studied. Three types of synthetic mica at three concentrations (2.5, 5.0, and 7.5 wt % mica) were used and the effect of these micas on the crystallization and thermal properties of PLA was investigated by differential scanning calorimetry (DSC). The Avrami and Hoffman-Weeks equations were used to describe the isothermal crystallization kinetics and melting behavior. Addition of these micas to the PLA matrix increased the crystallization rate, and this effect depended on the mica type and concentration. While the nonmodified Somasif ME-100 exerted the smallest effect, the effect observed for the organically modified Somasif MPE was the most pronounced. The lower half-time of crystallization $t_{1/2}$ was around 3 min for the PLA/Somasif MPE nanocomposites containing 7.5 wt % of filler at 90°C, which is about 16 min below that found for neat PLA. The equilibrium melting temperature (T_m°) of PLA were estimated for these systems, showing an increase in the composites and an increase with increasing loading, except for PLA/Somasif MPE, in which the increase of the mica content decreased T_m° about 5°C. © 2014 Wiley Periodicals, Inc. J. Appl. Polym. Sci. **2014**, *131*, 40322.

KEYWORDS: biodegradable; nanostructured polymers; polyesters; crystallization; clay

Received 4 October 2013; accepted 17 December 2013
DOI: 10.1002/app.40322

INTRODUCTION

Poly(lactic acid) (PLA) has attracted great attention, particularly due to its production from renewable resources.[1] It has good mechanical properties, thermal plasticity, biodegradability, and biocompatibility, being thus a promising polymer for various end-use applications.[2–4]

For polymers, the control of their crystallization allows designing materials with required properties. However, the slow crystallization rate of PLA strongly hinders its development. In general, three main routes are used to accelerate the crystallization process of polymers.[5] The first one is to add a nucleating agent that will lower the surface free energy barrier, which induces nucleation, initiating crystallization at higher temperatures upon cooling. A second possibility is to add a plasticizer, which will increase the polymer chain mobility, enhancing the crystallization rate by reducing the energy required for the chain folding process. The third possibility is to change the molding conditions, in particular molding temperature and cooling time.[6]

In the past decades, many researchers have studied the crystallization behavior of PLA.[1,4–22] It is well understood that some inorganic fillers (clay, carbon nanotubes, calcium carbonate, etc.) which act as reinforcing agents in polymer composites can usually induce nucleation for the matrix crystallization[21,23–25] and accelerate the overall crystallization process.

Synthetic layered silicates consist of a very interesting class of fillers because of their high purity, low cost, and because they are commercialized with several intercalants. In the preparation of nanocomposites, this last feature may contribute to an adequate choice of the product, to favor a better interaction with the polymeric matrix. In previous publications, we have reported on the morphology, rheology and thermal behavior of PLA/Somasif mica nanocomposites.[26–28] However, although the crystallization kinetics of PLA was investigated by some authors, no study was reported on the crystallization of PLA induced by the nucleating effect of this type of synthetic mica. For this reason, the aim of this work was to study the crystallization behavior of PLA/Somasif synthetic mica systems from the melt under isothermal condition, in order to evaluate the influence of the intercalant on the crystallization kinetics.

EXPERIMENTAL

Materials

Poly(L-lactic acid) (PLA) Ingeo 2002D from NatureWorks was used to prepare the nanocomposites. This PLA has a $T_g = 58$°C and relatively low T_m (151°C) due to the presence of D-lactic acid

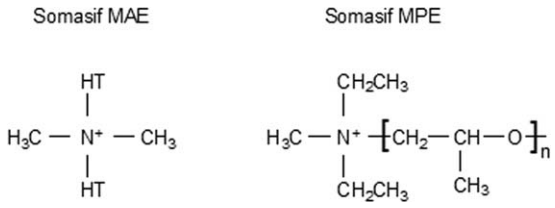

Figure 1. Intercalant structure of Somasif MAE and MPE.

unities. Three different synthetic fluoromicas (Somasif ME-100, MAE, and MPE) were obtained from CO-Op Chemical Co. Somasif ME-100 is a hydrophilic swellable mica with a cation-exchange capacity (CEC) of 120 meq/100 g. Somasif MAE and Somasif MPE are organomodified fluoromicas containing a dimethyl dihydrogenated tallow ammonium chloride (2M2HTA) and a methyl-diethyl-polypropylene glycol ammonium (M2EPG) as intercalant, respectively (Figure 1), where HT are hydrogenated hydrocarbon linear chains, with typical composition C18: 65%, C16: 30%, and C14: 5%.[29,30] According to the manufacturer, the Somasif mica have the general chemical composition: $(Na)_{2x}(Mg)_{3-x}(Si_4O_{10})(F_yOH_{1-y})_2 \cdot nH_2O$, where $0.15 < x < 0.5$; $0.8 < y < 1.0$.

Sample Preparation

In order to eliminate PLA moisture, before processing, the polyester was dried for 4 h at 90°C in a vacuum oven. The synthetic micas, which are also capable of absorbing moisture, were dried under the same conditions.

PLA/Somasif mica nanocomposites with different clay loadings (2.5, 5.0, and 7.5 wt % mica) were prepared in a Coperion ZSK 18 (Werner & Pfleiderer GmbH & Co. KG, Stuttgart, Germany) co-rotating twin-screw extruder, with L/D ratio of 40, at temperatures in the range of 180 to 200°C, and screw speed set at 120 rpm. Pristine PLA was also processed under the same conditions for comparison purposes.

Isothermal Crystallization

Differential scanning calorimetry (DSC) analysis was used to study the isothermal crystallization behavior and thermal properties of PLA and PLA/synthetic mica nanocomposites. A Perkin-Elmer DSC 7 was used. A sample of about 13 mg was first heated from 30 to 180°C at 20°C/min and held for 3 min to erase the thermal history, and then it was cooled at 100°C/min to the prescribed crystallization temperature (90–120°C) and held for enough time to fully crystallize, then cooled at the

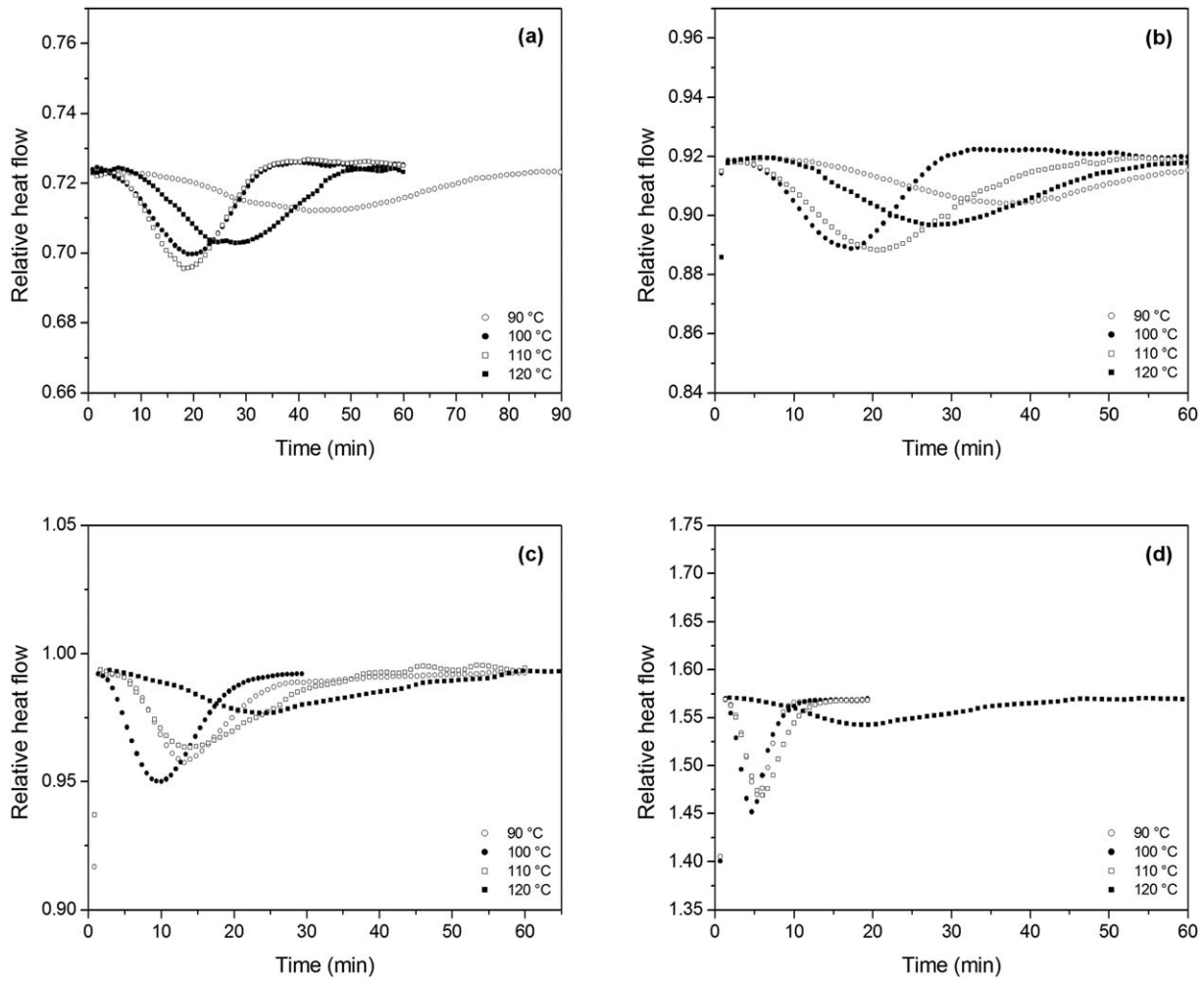

Figure 2. DSC curves of isothermal crystallization at different temperatures for (a) PLA and nanocomposites with 2.5 wt % of mica: (b) PLA/Somasif ME-100, (c) PLA/Somasif MAE and (d) PLA/Somasif MPE.

same rate to 30°C and held for 3 min. Finally, the sample was heated again to 180°C at 10°C/min to get T_m. The analyses were carried out under nitrogen atmosphere using a flow rate of 20 mL/min.

RESULTS AND DISCUSSION

Isothermal Crystallization

Isothermal melt-crystallization of PLA and various PLA-synthetic mica nanocomposites were investigated at four crystallization temperatures, 90, 100, 110, and 120°C.

The morphology of these PLA-synthetic mica composites investigated by SAXS and TEM were described in our previous publications,[27,28,31] which demonstrated that, particularly in the case of organo-modified synthetic micas, particles are dispersed in a nanometer scale, forming tactoids with thickness from 20 to 90 nm in filler concentration up to 5 wt %. At higher mica contents, both mica nanodomains and microdomains were found.

Figure 2 shows the isothermal crystallization exotherms of PLA (a), PLA/Somasif ME-100 (b), PLA/Somasif MAE (c), and PLA/Somasif MPE (d) with 2.5 wt % of synthetic mica. According to the exothermic peaks, the addition of mica into the PLA matrix has a significant effect on the crystallization behavior of the material. When Somasif ME-100 is added, the improvement in crystallization is mild, but when the organomodified micas are present in the matrix, a dramatic change in the crystallization profile is observed, with complete crystallization taking place in significantly shorter times. According to our previous published papers, the introduction of non-organomodified synthetic mica lead to predominant microdomains of the filler, differently of what takes place for the organomodified micas, in which nanodomains are predominant. This means that the size of the mica entities in PLA is smaller when using the organomodified mica, because the organic intercalant favor exfoliation of mica microaggregates, resulting in a nanostructured material. Since mica is known to act as nucleating agents, this means that the number of crystalline entities probably increased in presence of these nanostructures and consequently the crystallization rate also increased. While PLA has its fastest complete crystallization at around 35 min, the nanocomposites with organomodified micas have taken 10 to 15 min to crystallize completely.

Comparing both organomodified synthetic micas, Somasif MPE has the higher effect on the crystallization behavior than Somasif MAE. Li and Huneault have investigated the effect of plasticizers in the crystallization behavior of PLA containing different known nucleating agent and plasticizers and showed that the adequate combination of nucleation and plasticization resulted in significant development of crystallinity even at high cooling rates. The effect was explained considering the increase in the PLA chain mobility.[32] Thus, once Somasif MPE has higher amount of organic intercalant (around 66 wt %),[26] it is probable that the intercalants also acting in our case as a plasticizer, giving more mobility to PLA chains, which may facilitate crystallization.

Effect of Mica Content

Figure 3 shows the crystallization exotherms of PLA and their synthetic mica nanocomposites at different compositions,

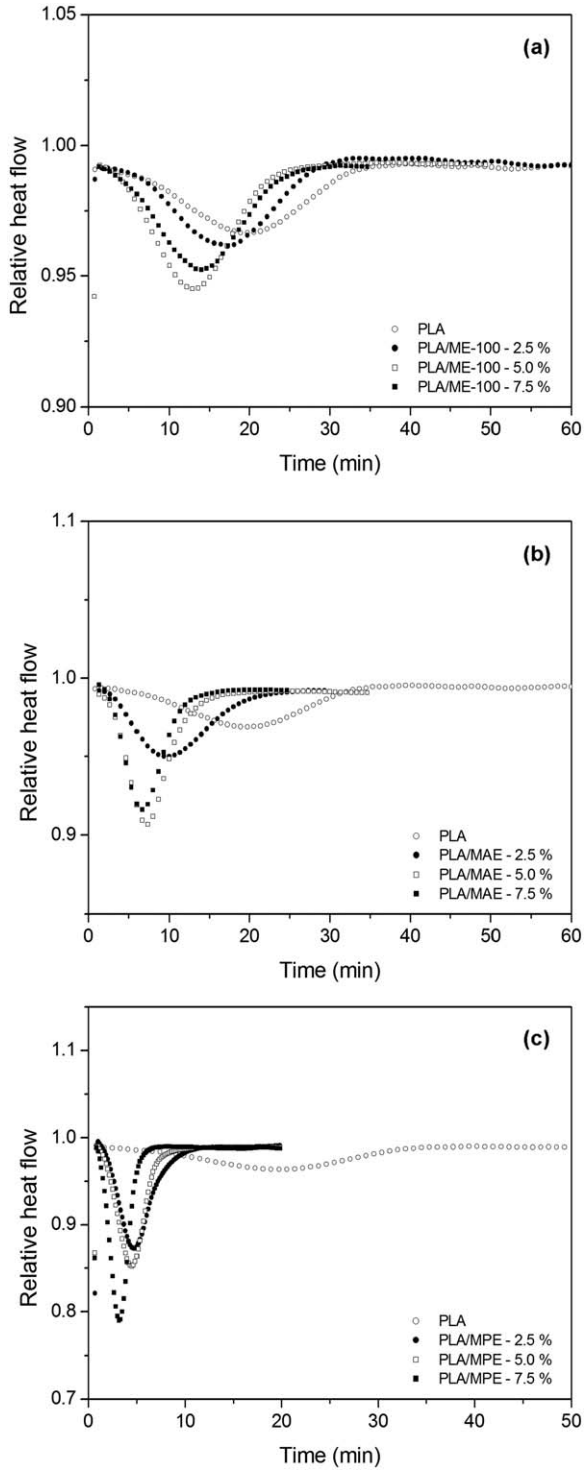

Figure 3. DSC curves of isothermal crystallization at 100°C for (a) PLA/Somasif ME-100, (b) PLA/Somasif MAE, and (c) PLA/Somasif MPE nanocomposites.

isothermally crystallized at 100°C. As observed for the effect of mica type, these results show that total crystallization of PLA/synthetic mica nanocomposites has taken place at shorter times as compared to PLA. As mica content increases, the time for complete crystallization decreases. Similar behavior was also observed at the other crystallization temperatures used in this

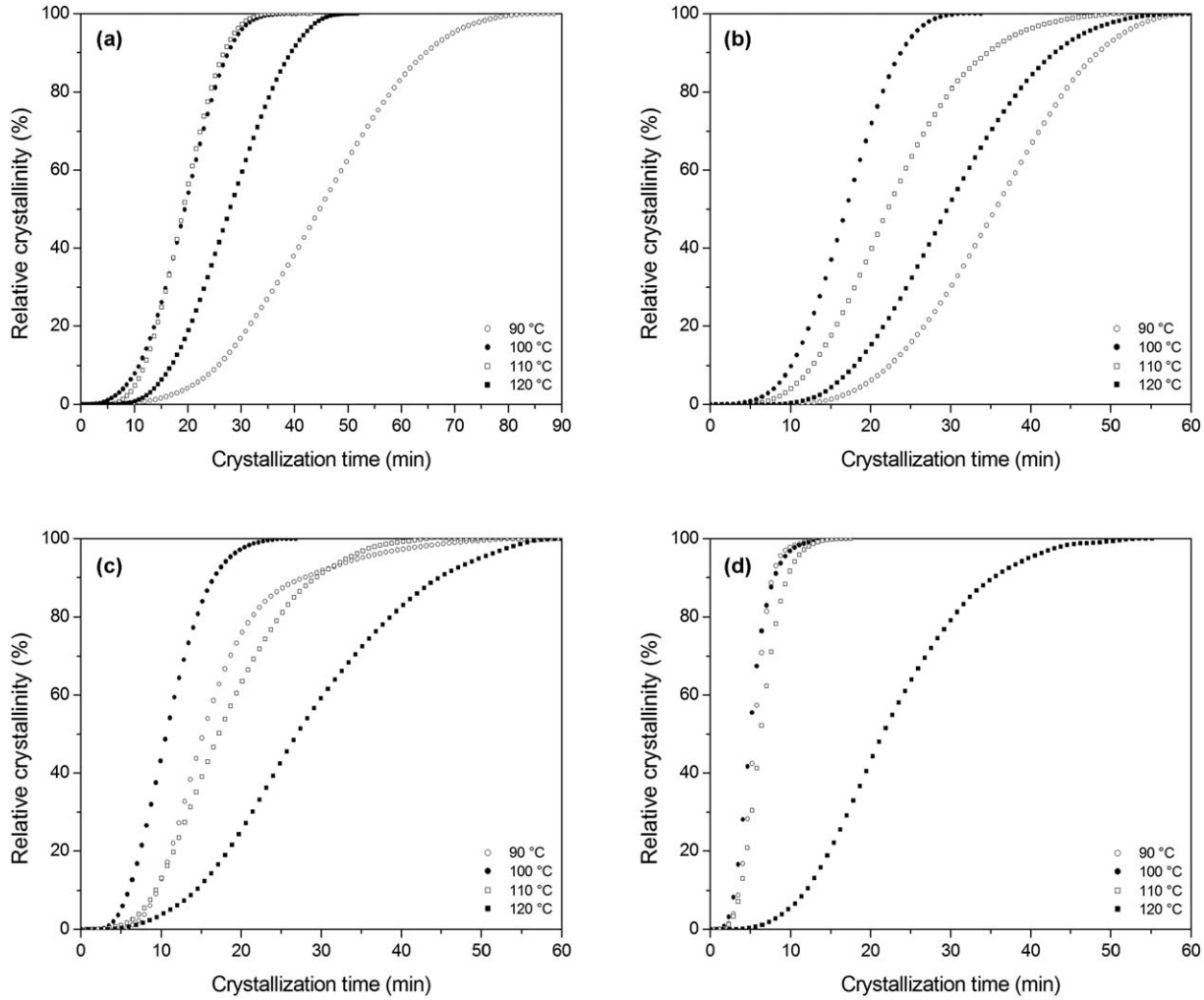

Figure 4. Relative crystallinity versus time at various crystallization temperatures for (a) PLA and nanocomposites with 2.5 wt % of mica: (b) PLA/Somasif ME-100, (c) PLA/Somasif MAE, and (d) PLA/Somasif MPE.

work (90, 110, and 120°C). The effect of increasing the crystallization rate with increasing filler concentration is expected since mica particles enhance the rate of crystallization by heterogeneous nucleation, which occurs at preferential sites and provides new surfaces on which crystal growth can occur. The heterogeneous nucleation takes place because the lower effective surface energy decreases the free energy barrier, facilitating nucleation.

Effect of Temperature

The isothermal crystallization kinetics can be better visualized by evaluating the degree of crystalline conversion as a function of time at a constant temperature. The relative crystallinity at different crystallization time, α, can be calculated according to the following equation:

$$\propto = \frac{\int_0^t (dH/dt)dt}{\int_0^\infty (dH/dt)dt}$$

where (dH/dt) is the DSC heat flow rate. The relative crystallinity versus crystallization time for PLA, PLA/Somasif ME-100, PLA/Somasif MAE and PLA/Somasif MPE with 2.5 wt % of mica had been plotted in Figure 4, respectively.

From Figure 4(a), it was found that PLA has the fastest crystallization rate between 100 and 110°C, and it takes a long time to crystallize at 90°C. When Somasif ME-100 is added [Figure 4(b)], this behavior is maintained for all compositions. Figure 4(c,d) show the crystallization behavior for the nanocomposites containing the organomodified micas. It can be noted that the fastest crystallization rate also occurs at 100°C. At 120°C, it takes the longest time, which means that the crystallization rate decreases.

The crystallization kinetics of PLA and its nanocomposites under isothermal crystallization were analyzed by the Avrami equation:[33–35]

$$\propto = 1 - \exp(-kt^n)$$

where k is the crystallization rate constant and n is the Avrami exponent whose value depends on the mechanism of nucleation and on the form of crystal growth. Figure 5 presents $\ln[-\ln(1-\alpha)]$ versus $\ln\ t$ plots for the neat PLA and the

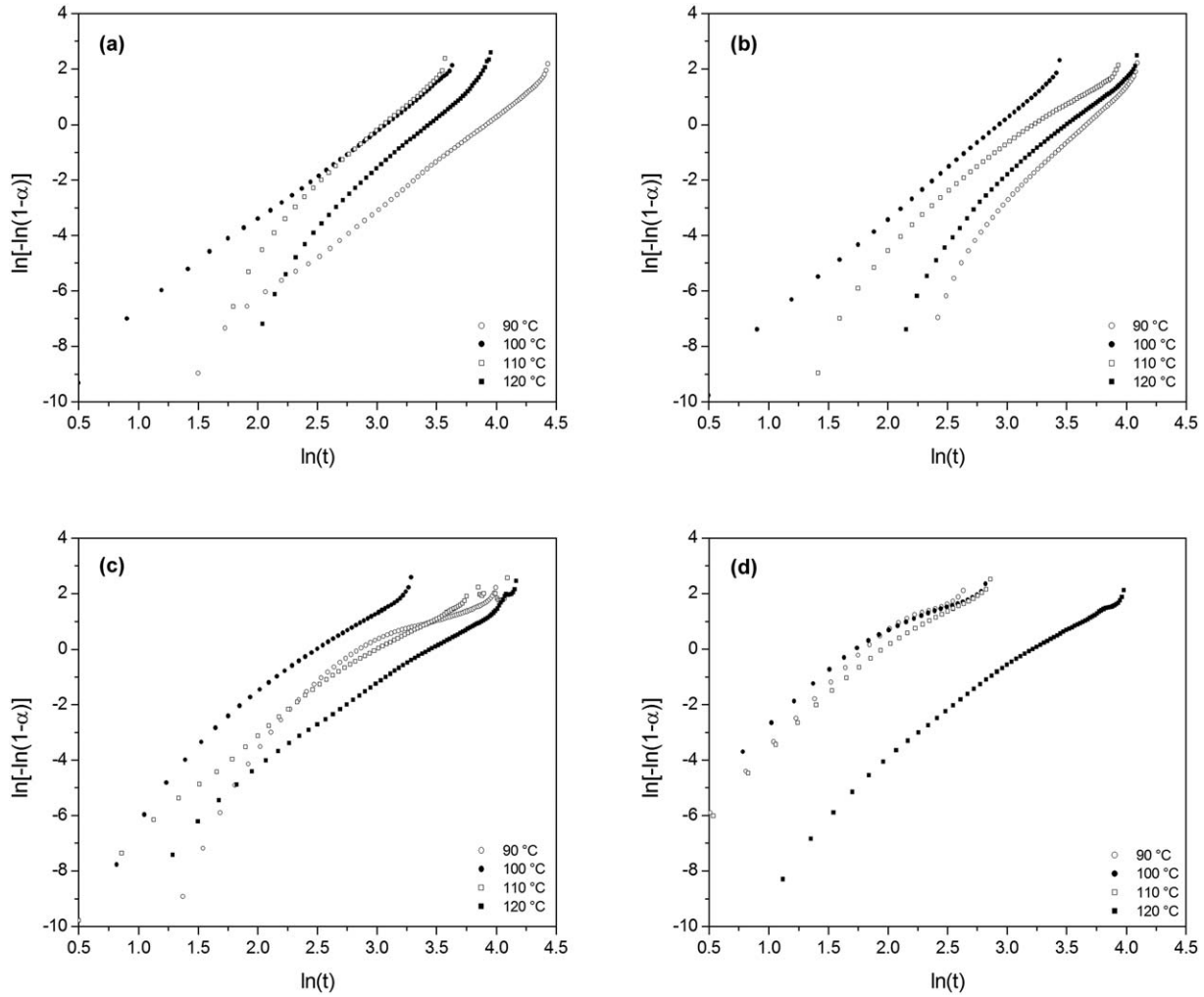

Figure 5. Avrami analysis for (a) PLA and (b) PLA/Somasif ME-100, (c) PLA/Somasif MAE, and (d) PLA/Somasif MPE nanocomposites with 2.5 wt % of mica isothermally crystallized at various crystallization temperatures.

PLA/synthetic mica nanocomposites at different crystallization temperatures.

The data obtained from the plots and Avrami equation are listed in Table I. The Avrami exponents obtained for neat PLA were in the range of 3 to 4. It implies that PLA crystals present spherulitic growth[7] under these experimental conditions. The addition of Somasif ME-100 did not change the geometry growth of the crystals formed. The PLA/Somasif MAE nanocomposites with 2.5 wt % of mica presented n in the range of 2 to 3, suggesting a disc-like growth. Nevertheless, when a higher amount of this synthetic mica is added to PLA, a spherulitic growth seems to be predominant according to n values. PLA/Somasif MPE also showed heterogeneous nucleation and spherulitic growth.

The half-time of crystallization $t_{1/2}$ is defined as the time to reach 50% crystallization. It is also used to directly characterize the crystallization rate, since the reciprocal half-time of crystallization $(1/t_{1/2})$ can be considered approximately proportional to the crystal growth rate (G).[9] It can be said that the longer the half-time of crystallization, the slower the crystallization rate. Furthermore, from n and k, $t_{1/2}$ can be obtained from:

$$t_{1/2} = \left(\frac{ln2}{k}\right)^{1/n}$$

Table I shows the half-time of crystallization calculated by the equation above and those estimated from the relative crystallinity versus crystallization time plots. The table shows the $t_{1/2}$ data obtained from both techniques are in accordance with each other. PLA/Somasif MPE nanocomposite had the lowest half-time of crystallization. The best crystallization temperature for neat PLA was 100°C when $t_{1/2}$ is around 19 min. Among the nanocomposites, the higher crystallization rate is attained for PLA/Somasif MPE with 7.5 wt % of mica in which $t_{1/2}$= 3.1 min was obtained at 90°C.

Equilibrium Melting Temperature

Table II presents the melting temperature peaks of PLA and PLA/synthetic mica nanocomposites after the isothermal crystallization at various temperatures. Either single or double melting peaks were observed in the DSC curves. The low and high melting temperatures were labeled as T_{m1} and T_{m2}, respectively. T_{m1} values gradually were shifted to higher temperatures with increasing crystallization temperature. In contrast, T_{m2} values showed much

Table I. Avrami Kinetic Parameters for the Crystallization of PLA and the Various Nanocomposites

Material	T_c (°C)	n	ln(k)	k (s^{-n})	$t_{1/2}$ (min)	Calculated $t_{1/2}$ (min)
PLA	90	3.37	−13.19	1.87E-06	44.74	44.93
	100	3.19	−9.78	5.66E-05	19.43	19.12
	110	3.63	−11.10	1.51E-05	19.15	19.24
	120	3.51	−12.06	5.79E-06	21.92	27.98
PLA/ME-100-2.5%	90	3.94	−14.46	5.25E-07	35.63	35.77
	100	3.64	−10.69	2.28E-05	16.95	17.05
	110	2.81	−9.13	1.08E-04	22.19	22.62
	120	3.30	−11.59	9.26E-06	29.59	30.00
PLA/ME-100-5.0%	90	3.45	−12.46	3.88E-06	32.88	33.29
	100	3.38	−9.12	1.09E-04	13.21	13.33
	110	3.21	−9.38	8.44E-05	16.41	16.58
	120	3.42	−11.25	1.30E-05	24.09	24.10
PLA/ME-100-7.5%	90	3.81	−13.03	2.19E-06	27.56	27.76
	100	3.36	−9.27	9.42E-05	14.03	14.15
	110	3.35	−9.09	1.13E-04	13.29	13.52
	120	3.34	−10.83	1.98E-05	22.77	22.94
PLA/MAE-2.5%	90	3.00	−8.62	1.80E-04	15.24	15.66
	100	2.73	−6.84	1.07E-03	10.64	10.71
	110	2.4	−7.23	7.25E-04	17.20	17.46
	120	2.42	−8.37	2.32E-04	27.02	27.31
PLA/MAE-5.0%	90	5.52	−11.22	1.34E-05	7.47	7.14
	100	4.29	−8.99	1.25E-04	7.57	7.46
	110	3.76	−9.47	7.71E-05	11.43	11.26
	120	3.18	−10.76	2.12E-05	25.76	26.27
PLA/MAE-7.5%	90	5.11	−10.40	3.04E-05	7.54	7.12
	100	3.86	−7.9	3.71E-04	7.05	7.04
	110	4.01	−9.25	9.61E-05	9.31	9.16
	120	3.42	−11.28	1.26E-05	24.97	24.31
PLA/MPE-2.5%	90	4.4	−7.89	3.74E-04	5.55	5.53
	100	4.02	−6.81	1.10E-03	5.01	4.97
	110	3.88	−7.3	6.76E-04	6.30	5.97
	120	2.43	−7.82	4.02E-04	21.55	21.48
PLA/MPE-5.0%	90	4.34	−7.04	8.76E-04	4.66	4.65
	100	3.93	−6.23	1.97E-03	4.46	4.45
	110	3.89	−7.73	4.39E-04	6.73	6.64
	120	2.74	−9	1.23E-04	23.60	23.36
PLA/MPE-7.5%	90	3.97	−4.87	7.67E-03	3.09	3.11
	100	4.21	−5.3	4.99E-03	3.21	3.23
	110	3.73	−6.95	9.59E-04	5.85	5.84
	120	4.22	−13.8	1.02E-06	25.69	24.13

less dependence on the isothermal crystallization temperature. The double-melting behavior of isothermally crystallized PLA has been reported in literature, and assigned to melt-recrystallization by Yasuniwa et al.,[36] or to the possible degradation of PLA melt by Wang and Mano.[37] T_{m1} is attributed to primary crystallites formed at T_c, with T_{m2} reflecting the relatively perfect lamella stacks resulted from recrystallization during the heating scan.[38]

In order to determine the T_m° of PLA, T_m values corresponding to the lower-temperature endothermic peak (T_{m1}) were used. According to the theoretical consideration by Hoffman and Weeks, the equilibrium melting point temperature can be obtained by linear extrapolation of the T_m versus T_c plot to the line $T_m = T_c$, and the dependence of the T_m on the T_c is given by

Table II. Transition Temperatures, Enthalpies, and Degree of Crystallization of PLA and PLA/Synthetic Mica Nanocomposites

Material	T_c (°C)	T_{m1} (°C)	T_{m2} (°C)	ΔH_m (J/g)	ΔH_c (J/g)	ΔH_p (J/g)	X_c (%)
PLA	90	143.1	155.1	31.0	27.0	-	29.2
	100	146.6	154.4	33.5	28.5	-	31.7
	110	149.8	153.9	33.8	26.4	-	31.9
	120	153.1	-	37.9	30.1	-	35.7
PLA/ME-100-2.5%	90	144.5	156.7	29.5	20.8	30.3	28.5
	100	147.2	155.1	34.4	25.7	35.3	33.3
	110	150.1	154.5	33.7	36.9	34.5	32.6
	120	154.3	-	38.2	33.1	39.1	36.9
PLA/ME-100-5.0%	90	143.3	155.2	27.1	27.5	27.7	26.2
	100	147.1	155.4	37.1	31.8	38.0	35.9
	110	150.3	156.1	34.1	31.3	35.0	33.0
	120	153.3	-	37.7	38.0	38.7	36.5
PLA/ME-100-7.5%	90	143.0	155.4	30.1	17.9	30.9	29.1
	100	147.9	156.4	32.9	27.7	33.8	31.9
	110	150.9	157.2	36.1	30.0	37.1	35.0
	120	153.4	-	38.2	33.1	39.2	36.9
PLA/MAE-2.5%	90	144.4	157.0	30.7	26.5	32.1	30.3
	100	149.1	158.2	33.1	26.0	34.5	32.6
	110	152.9	159.0	38.6	33.6	40.3	38.0
	120	153.9	-	38.3	27.7	40.0	37.8
PLA/MAE-5.0%	90	143.7	156.4	32.9	25.7	35.9	33.9
	100	147.0	155.8	34.6	29.2	37.8	35.7
	110	149.9	156.7	38.0	32.3	41.5	39.2
	120	153.7	-	37.3	27.1	40.8	38.5
PLA/MAE-7.5%	90	141.9	156.3	28.1	23.6	32.2	30.4
	100	148.0	157.0	30.9	26.3	35.4	33.4
	110	149.4	155.7	36.2	30.2	41.5	39.1
	120	152.5	-	35.3	37.9	40.5	38.2
PLA/MPE-2.5%	90	142.8	154.6	25.1	23.2	27.1	25.6
	100	146.1	155.4	34.7	30.1	37.4	35.3
	110	149.7	157.2	35.7	32.1	38.6	36.4
	120	153.5	-	38.7	35.7	41.8	39.4
PLA/MPE-5.0%	90	142.0	154.2	30.7	27.1	36.1	34.0
	100	144.3	154.0	31.4	27.9	36.9	34.8
	110	147.4	154.9	36.8	34.3	43.2	40.7
	120	151.3	155.4	37.7	34.6	44.3	41.7
PLA/MPE-7.5%	90	140.5	152.6	30.6	24.5	39.3	37.1
	100	142.7	152.7	32.2	27.3	41.4	39.0
	110	146.5	154.4	34.0	31.2	43.7	41.3
	120	150.2	154.7	38.0	36.7	48.8	46.0

$$T_m = T_m^0\left(1-\frac{1}{\gamma}\right)+\left(\frac{T_c}{\gamma}\right)$$

where γ is the thickening ratio.[39]

As a typical example of the curves obtained, the T_m versus T_c data for the neat PLA and composites containing 2.5 wt % of each mica is plotted in Figure 6. The equilibrium melting points obtained for all materials at the different micaÇs concentration are presented in Table III.

The equilibrium melting temperature for neat PLA obtained from Figure 6(a) was 169.5°C that is in the range of values reported in the literature (166–225°C).[7,9,11,12,20,30–46] It means that for this PLA which contains about 2% of D-units this is

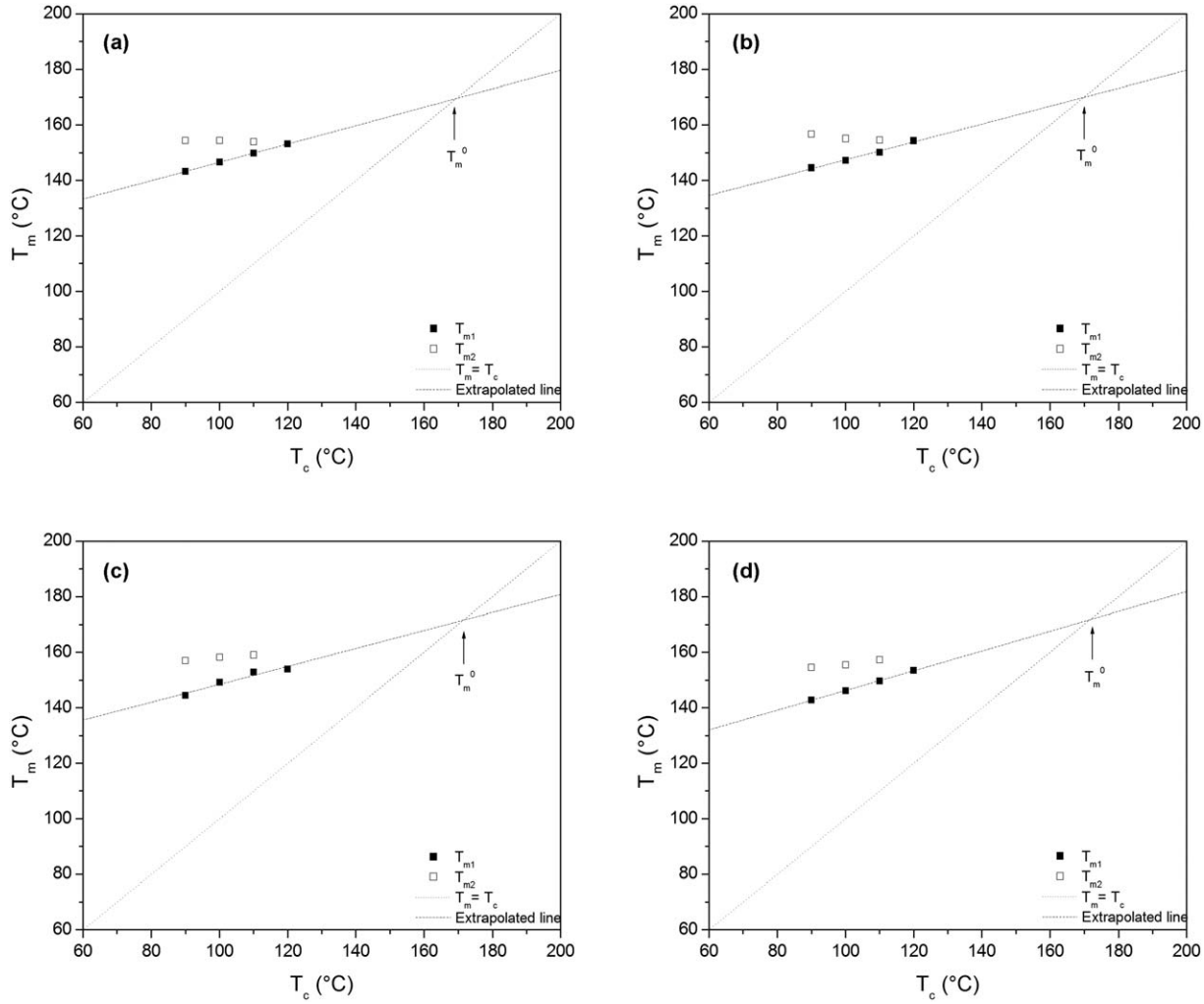

Figure 6. Melting-crystallization temperature curves and determination of the equilibrium melting point for PLA (a) and PLA/Somasif ME-100 (b), PLA/Somasif MAE (c), PLA/Somasif MPE (d) nanocomposites with 2.5 wt %.

the T_m value for crystals with the most perfect lamellae or, according to the theory derived by Hoffman and Weeks, the melting temperature of infinitely extended crystals of this polymer. We have found different values of T_m° for the composites, depending on the mica type and composition. In general, addition of mica into the PLA matrix slightly increased T_m° which may imply in more perfect or ticker lamellae crystals. The T_m° values increased as the content of non-modified sodium mica increased. However, this behavior was not observed when the organomodified fluoromica content increased. For PLA/MAE and PLA/MPE nanocomposites the T_m° value are higher than that observed for the neat PLA, but decreased with increasing mica content. Similar behavior for PA-6/multiwalled carbon nanotubes nanocomposites was previously reported and attributed to induction of the formation of various crystalline structures.[45] For the PLA/organomodified synthetic mica systems of this work, even observing an increase in the crystallization rate, it seems the intercalant of those micas acts in such way that a reduction in the lamellae thickness of the PLA crystals takes place. The reduction in T_m° with increasing mica content is more pronounced for the PLA/Somasif MPE nanocomoposites, probably due to the large amount of intercalant present in this mica.

Table III. Equilibrium Melting Temperature of PLA and PLA/Synthetic Mica Nanocomposites

Material	Mica content (%)	T_m° (°C)
PLA	0	169.5
PLA/ME-100	2.5	170.0
	5.0	170.1
	7.5	171.5
PLA/MAE	2.5	171.6
	5.0	170.0
	7.5	169.5
PLA/MPE	2.5	171.8
	5.0	164.8
	7.5	164.6

The equilibrium melting point of PLA found in this work is low compared to literature most commonly reported data (higher than 200°C). The main reason for the low equilibrium melting point is not the low molecular weight but the low optical purity of PLLA.

CONCLUSIONS

The isothermal crystallization kinetics of nanocomposites of PLA and three synthetic Somasif micas (Somasif ME-100, Somasif MAE, and Somasif MPE) was studied by DSC. The synthetic micas were blended with PLA at different contents (2.5, 5.0, and 7.5 wt % mica). The incorporation of the synthetic micas significantly accelerates the crystallization process of the PLA matrix as expected. This effect is more pronounced when Somasif MPE is added to the biodegradable polymer. As mica content increases shorter crystallization times is needed to attain the complete crystallization of PLA matrix. The nanocomposites with organomodified micas took 10 to 15 min to crystallize completely while PLA has taken around 35 min. The maximum crystallization rate is reached with the crystallization temperature of 90°C for the PLA/Somasif MPE nanocomposites with 7.5 wt % of mica.

ACKNOWLEDGMENTS

The authors are grateful to CNPq, CAPES, and FAPERJ for the financial support.

REFERENCES

1. Kawai, T.; Rahman, N; Matsuba, G.; Nishida, K.; Kanaya, T.; Nakano, M.; Okamoto, H.; Kawada, A.; Usuki, J.; Honma, N.; Nakajima, K.; Matsuda, M. *Macromolecules* **2007**, *40*, 9463.
2. Tsuji, H.; Ikada, Y. *J. Appl. Polym. Sci.* **1998**, *67*, 405.
3. Martin, O.; Avérous, L. *Polymer* **2001**, *42*, 6209.
4. Xiao, H.; Yang, L.; Ren, X.; Jiang, T.; Yeh, J. -T. *Polym. Compos.* **2010**, *31*, 2057.
5. Yasuniwa, M.; Tsubakihara, S.; Iura, K.; Ono, Y.; Dan, Y.; Takahashi, K. *Polymer* **2006**, *47*, 7554.
6. Battegazzore, D.; Bocchini, S.; Frache, A. *Express Polym. Lett.* **2010**, *5*, 849.
7. Kolstad, J. J. *J. Appl. Polym. Sci.* **1996**, *62*, 1079.
8. Urbanovici, E.; Schneider, H. A.; Brizzolara, D.; Cantow, H. J. *J. Therm. Anal. Calorimetry* **1996**, *47*, 931.
9. Iannace, S.; Nicolais, L. *J. Appl. Polym. Sci.* **1997**, *64*, 911.
10. Miyata, T.; Masuko, T. *Polymer* **1998**, *39*, 5515.
11. Di Lorenzo, M. L. *Polymer* **2001**, *42*, 9441.
12. Abe, H.; Kikkawa, Y.; Inoue, Y.; Doi, Y. *Biomacromolecules* **2001**, *2*, 1007–1014.
13. Kikkawa, Y.; Abe, H.; Iwata, T.; Inoue, Y.; Doi, Y. *Biomacromolecules* **2001**, *2*, 940.
14. Urayamaa, H.; Kanamori, T.; Fukushima, K.;Kimura, Y. *Polymer* **2003**, *44*, 5635.
15. Tsuji, H.; Tezuka, Y. *Biomacromolecules* **2004**, *5*, 1181.
16. Zhang, J.; Tsuji, H.; Noda, I.; Ozaki, Y. *Macromolecules* **2004**, *37*, 6433.
17. Mano, J. F.; Wang, Y. M.; Viana, J. C.; Denchev, Z.; Oliveira, M. J. *Macromol. Mater. Eng.* **2004**, *289*, 910.
18. Di Lorenzo, M. L. *Eur. Polym. J.* **2005**, *41*, 569.
19. He, Y.; Fan, Z. Y.; Hu, Y. F.; Wu, T.; Wei, J.; Li, S. M. *Eur. Polym. J.* **2007**, *43*, 4431.
20. Liao, R.; Yang, B.; Yu, W.; C. Zhou, *J. Appl. Polym. Sci.* **2007**, *104*, 310.
21. Su, Z.; Guo, W.; Liu, Y.; Li, Q.; Wu, C. *Polym. Bull.* **2009**, *62*, 629.
22. Tábi, T.; Sajó, I. E.; Szabó, F.; Luyt, A. S.; Kovács, J. G. *Express Polym. Lett.* **2010**, *4*, 659.
23. Fornes, T. D.; Paul, D. R. *Polymer* **2003**, *44*, 3945.
24. Grozdanov, A.; Buzarovska, A.; Bogoeva-Gaceva, G.; Nedkov, E. *J. Polym. Sci. Part B: Polym Phys* **2005**, *43*, 66.
25. Wang, B.; Sun, G.; Liu, J.; He, X.; Li, J. *J. Appl. Polym. Sci.* **2006**, *100*, 3794.
26. Souza, D. H. S.; Dahmouche, K.; Andrade, C. T.; Dias, M. L. *Appl. Clay Sci.* **2011**, *54*, 226.
27. Souza, D.H.S.; Dahmouche, K.; Dias, M.L.; Andrade, C.T. *Appl. Clay Sci.* **2013**, *80*, 259.
28. Souza, D. H. S., Andrade C. T., Dias M. L., *Mater. Sci. Eng. C Mater. Biol. Appl.* **2013**, *33*, 1795.
29. Souza, D. H. S. PhD Thesis; Rio de Janeiro, Brazil: Universidade Federal do Rio de Janeiro, **2011**.
30. Bordes, P.; Pollet, E.; Avérous, L. *Prog. Polym. Sci.* **2009**, *34*, 125.
31. Borges, S. V.; Dias, M. L.; Pita, V. J. R. R.; Azuma, C. V.; Dias, M.V. *J. Plast. Film Sheet* **2012**, *28*, 1.
32. Li, H., Huneault, M. A. *Polymer* **2007**, *48*, 6855.
33. Avrami, M. *J. Chem. Phys.* **1939**, *7*, 1103.
34. Avrami, M. *J. Chem. Phys.* **1940**, *8*, 212.
35. Avrami, M. *J. Chem. Phys.* **1941**, *9*, 177.
36. Yasuniwa, M.; Tsubakihara, S.; Sugimoto, Y.; Nakafuku, C. *J. Polym. Sci. Part B: Polym. Phys.* **2004**, *42*, 25.
37. Wang, Y. M.; Mano, J. F. *Eur. Polym. J.* **2005**, *41*, 2335.
38. Hea, Y.; Fana, F.; Hua, Y.; Wua, T.; Weia, J.; Lia, B. *Eur. Polym. J.* **2007**, *43*, 4431.
39. Hoffman, J. D.; Weeks, J. J. *J. Res. Nat. Bur. Stand* **1962**, *66*, 13.
40. Marand, H.; Xu, J.; Srinivas, S. *Macromolecules* **1998**, *31*, 8219.
41. Nam, J. Y.; Ray S. S.; Okamoto, M. *Macromolecules* **2003**, *36*, 7126.
42. Cho, J.; Baratian, S.; Kim, J.; Yeh, F.; Hsiao, B. S.; Runt, J. *Polymer* **2003**, *44*, 711.
43. Teramoto, Y.; Nishio, Y. *Biomacromolecules* **2004**, *5*, 397.
44. Lee, S.-H.; Wang, S.; Teramoto, Y. *J. Appl. Polym. Sci.* **2008**, *108*, 870.
45. Li, X.; Yin, J.; Yu, Z.; Yan, S.; Lu, X.; Wang, Y.; Cao, B.; Chen, X. *Polym. Compos.* **2009**, *30*, 1338.
46. Li, J. Fang, Z., Zhu, Y.; Tong L.; Gu, A.; Liu, F. *J. Appl. Polym. Sci.* **2007**, *105*, 3531.